REVIEW ARTICLE

Ground-Based Augmentation Systems Operation in Low Latitudes - Part 1: Challenges, Mitigations, and Future Prospects

Leonardo Marini-Pereira[1],* [iD], Sam Pullen[2] [iD], Alison de Oliveira Moraes[3] [iD], Jonas Sousasantos[4] [iD]

1. Departamento de Controle do Espaço Aéreo – Instituto de Controle do Espaço Aéreo – Divisão de Pesquisa – São José dos Campos/SP – Brazil. 2.Stanford University – Department of Aeronautics and Astronautics – Stanford/CA – United States of America. 3.Departamento de Ciência e Tecnologia Aeroespacial – Instituto de Aeronáutica e Espaço – Divisão de Eletrônica – São José dos Campos/SP – Brazil. 4.Departamento de Ciência e Tecnologia Aeroespacial – Instituto Tecnológico de Aeronáutica – Divisão de Ciência da Computação – São José dos Campos/SP – Brazil.

*Correspondence author: marinilmp@fab.mil.br

ABSTRACT

Ground-based augmentation systems (GBASs) were designed to support civil aviation precision approach and landing with safety and integrity. It has several advantages over traditional navigation aids, allowing airspace usage optimization and reduction of fuel consumption. However, in low-latitude regions such as Brazil, this technology is still not operational due to the strong influence of ionospheric variability. Considering the increased interest in deploying a GBAS station in Brazil along with efforts toward this goal over the last decade, this paper is the first of a two-part series that provides an overview of the key aspects of this technology and the challenges posed when using it in low-latitude regions. The context in which GBAS operates today in midlatitudes is presented along with its fundamental principles and methods of guaranteeing sufficient accuracy, continuity, and integrity for precision operations, particularly those dealing with threatening ionospheric conditions. Finally, the evolution of GBAS to include multiple Global Navigation Satellite System (GNSS) satellite constellations and signal frequencies are discussed with respect to their ability to mitigate ionospheric effects. The conclusion is that the use of these new elements of GBAS seem to be the most viable solution for operating GBAS in low latitudes with high availability.

Keywords: GBAS; Ionosphere; Integrity; Air navigation.

INTRODUCTION

Satellite navigation

The use of satellite navigation by aircraft is a growing trend. Satellite navigation is widely used today by the worldwide aviation sector for all phases of flight. As aviation applications of satellite navigation proliferate, the demands on performance are continually increasing. The growth of navigation satellite numbers and signal performance is helping to meet these demands. As of early 2021, there are more than 100 navigation satellites orbiting around the Earth belonging to four different global constellations

(along with several regional constellations). These satellites broadcast more than 200 distinct signals, all devoted to providing positioning (GPS World 2021).

The use of Global Navigation Satellite System (GNSS) technology for air navigation has numerous advantages over conventional navigation, which is based on ground navigation aids used as references to define air routes, take-offs, and landing procedures. Conventional navigation has been used for decades but is less capable of meeting the increasing demands for optimal use of airspace and better navigation performance. In conventional navigation, the path of the aircraft is entirely dependent on locations of the navigation aids on the ground, resulting in very little airspace flexibility (ICAO 2020a). Additionally, maintenance of the extensive network of ground equipment, much of it fielded decades earlier, is complex and expensive.

In contrast, GNSS can make air navigation much more flexible, regardless of the position of ground equipment. In Brazil, GNSS-based air navigation procedures are widely used; 80% of all aerodromes that operate with instrument flight rules (IFR) have GNSS-based procedures, and more than 85% of airways are navigated by satellites (DECEA 2020). Considering the "approach" phase of flight, all GNSS-based procedures currently in operation in Brazilian airspace are classified as non-precision approach (NPA). This means they have lower performance and capability than those classified as precision approach (PA) and have restrictions in degraded visual conditions. For example, NPA approaches provide two-dimensional (2D) horizontal guidance only, whereas PA approaches add vertical guidance and allow aircraft to approach closer to the ground before regaining visibility.

To support PA and landing operations in severe meteorological conditions, conventional navigation has long used a traditional radio navigation aid known as the instrument landing system (ILS). Despite the popular use of ILS worldwide, technical restrictions and other constraints prevent its use at some airports. Instrument landing system has restrictions similar to conventional navigation aids and has a high cost of installation and maintenance with almost no flexibility in the path definitions for approach and landing procedures. The approach path provided by ILS is defined by radio signal patterns that depend entirely on the location of the antennas on the ground. For example, an ILS guides the navigation system of an aircraft to descent on a 3° angle with the runway (glide path angle [GPA]) until a touchdown point. Once the ILS is deployed and configured with this GPA for a specific touchdown point, these parameters are fixed and cannot be changed since they physically depend on the antennas on the ground. As a result, in case of temporary obstacles and restrictions or maintenance works on the runway, the approach procedures provided by the ILS would be put on halt, restricting access to the airport. Also, it must be noted that each ILS serves only runway end (direction) and hence, for an airport with one physical runway (two directions), two ILSs would be required to provide precision approaches for both. For two physical runways, four would be required and so on.

The Ground-Based Augmentation System [GBAS] Context

Technologies have been developed to improve satellite navigation performance by augmenting satellite positioning to provide "precision approach" services similar to those provided by ILS, but with additional benefits. This paper focuses on the GBAS, which is able to provide both high-accuracy aircraft positioning and substantial flexibility in the definition of landing procedures when compared to ILS. The advantages of GBAS over ILS include the use of a single ground facility to simultaneously provide information for multiple runways at the same aerodrome, the possibility of varying the approach glidepath (and thus supporting multiple touchdown points for the same runway end), and the possibility of curved approaches. In other words, GBAS provides precision approaches with all of the flexibility of GNSS-based navigation procedures.

A GBAS consists of a ground facility with multiple receivers installed at an airport tracking GNSS signals and using their known locations to calculate differential corrections for each healthy satellite (satellites determined to be unhealthy by the ground facility are excluded from use). These corrections are broadcast by a very high frequency (VHF) transmitter to the aircraft landing at that airport. Along with the corrections, the broadcast messages also carry uncertainty parameters that allow users to bound the errors in their navigation solution to very high probabilities, which contributes to the integrity and, thus, the safety of the system and the precision approach operation.

The ionospheric threat

Ionospheric refraction is one of the most significant influences on satellite positioning. The ionosphere is the layer of Earth atmosphere between 60 and 1,000 km above the surface, containing electrically-charged particles. Global Navigation Satellite System

satellites are typically at medium earth orbit (MEO), which means they orbit at more than 20,000 km of altitude. Satellite signals traversing the ionosphere suffer a refraction effect that changes the range to a satellite measured by a user below the ionosphere. Such effect results in position errors of different magnitudes, depending on the ionospheric condition.

For NPAs, the influence of ionospheric refraction in practical terms is negligible. Since NPAs use only the horizontal components of positioning and allow for errors of over 100 m, errors generated by even anomalous ionosphere have practically no impact on the safety of this kind of approach. However, for more stringent applications, like the use of GBAS for precision approaches, the influence of the ionosphere requires special treatment. This is due to the fact that precision approaches allow the aircraft to descend closer to the ground (200 ft or lower) without sight of the runway while relying entirely on the onboard navigation system. This closer proximity to the ground, the need for vertical guidance to give position relative to a glideslope, and the short amount of time to react in case a fault is encountered, or aircraft reaches the minimum altitude without regaining visual conditions place much greater demands on the integrity of GBAS. Henc it must provide a small error bound whose probability of being violated without annunciation is very low.

For this reason, the deployment of a GBAS station requires a thorough study of the ionospheric conditions in the region it will operate. In general, at regions farther from the Earth magnetic equator and outside of polar regions, the ionospheric impact on GBAS is manageable and allows it to provide at least 99% availability of precision approaches. However, in low-latitude regions (located between ± 25° of geomagnetic latitude), like Brazil, the ionosphere has complex dynamics and characteristics. Hence, high-availability GBAS operation in these regions is a huge challenge.

Motivation

The Brazilian Department of Airspace Control (DECEA), which is the regulatory authority and the air navigation service provider (ANSP) in Brazil, has been studying possibilities to deploy GNSS augmentation systems in Brazil over the last two decades. Around 2002, with the help of the United States Federal Aviation Agency (FAA), a satellite-based augmentation system (SBAS) testbed was installed and evaluated in the country with a few spread-out reference stations. That evaluation concluded that it would not be possible to use SBAS in Brazil for precision approach due to the strong influence of the ionosphere (ICAO 2002; 2006). The DECEA then turned its attention to the possibility of using GBAS instead.

In 2011, after the FAA had certified the Honeywell SLS-4000 GBAS ground facility for use in the Conterminous United States (CONUS), DECEA purchased a station and installed it at Rio de Janeiro International Airport (Galeão) to conduct trials and evaluate its viability for use in Brazil. The GBAS installation was completed in the same year at the beginning of the scintillation season and when the Sun 11-year activity cycle was increasing. Since it was not designed for this kind of environment, the ground station suffered unexpected alerts and shut-downs due to plasma-bubble occurrences in the ionosphere. For example, one of the GBAS monitors was programmed to exclude satellites with inconsistent measurements for 48 h, based on the assumption of a satellite fault. In the low-latitude environment, this monitor interpreted the scintillation effect as inconsistent measurements, and thus, all scintillating satellites were excluded for 48 h under the assumption of satellite fault. With multiple satellites not necessarily simultaneously affected by plasma bubbles, the GBAS monitor excluded a significant number of ranging sources resulting in less than minimum remaining satellites and the system shut-down.

In 2012, Honeywell started the development of a new software version for the SLS-4000 to better handle low-latitude ionosphere, among other issues. Among the new features, it was possible to configure a custom ionospheric threat model (as opposed to the fixed CONUS threat model originally included). A low-latitude ionospheric threat model (focused on Brazil) was developed by a multidisciplinary team from several organizations in Brazil, the U.S., and South Korea. The final results are described in Mirus Technology (2015), and discussed in Lee *et al*. (2015) and Yoon *et al*. (2017a). They show anomalous ionospheric gradients much larger than those in the CONUS threat model which affect the availability and the integrity of a GBAS in Brazil.

This multidisciplinary team also examined the operational conditions for the GBAS station in Rio de Janeiro, taking advantage of the configurable parameters of the station. The team concluded that GBAS operation would be safe only during local daytime hours, when the CONUS ionospheric threat model can be used (Chang *et al*. 2019; 2021). Due to this restriction (and other maintenance issues), Brazilian authorities decided not to certify the system for operations in Brazil. As a result, considering the

current limitations of both GBAS and SBAS, Brazil remains without any augmentation system to provide GNSS-based precision approaches and cannot benefit from such system.

The additional use of GPS L5 and Galileo E5 signals has the potential to mitigate ionospheric effects in real-time and thereby guarantee integrity for air navigation. Standards development for dual-frequency and multi-constellation SBAS and GBAS is underway to exploit this and other GNSS modernizations. However, the completion of standards and safety cases to use these enhancements in the aviation community is at least several years to a decade away.

Goals of this paper

This survey paper is the first of a two-part review series that presents the main challenges for implementing a GBAS station in Brazil due to the severe effects of low-latitude ionosphere. More broadly, it aims to clarify to those unfamiliar with the subject the main principles of GBAS technology and how the ionosphere over Brazil impacts the operation of a GBAS station. The most important aspects of low-latitude ionospheric behavior are explained and discussed in a subsequent paper (the second installment of this two-part series). Putting this information together provides a primary source of information for those who wish to have a complete overview of the problem. This compilation is based upon the experience of DECEA in studying and testing GBAS technology to evaluate its viability in Brazil. For readers interested in knowing more details about specific topics, the references cited herein are useful sources of information.

To accomplish this goal, a general overview of the categories of navigation that GBAS supports is provided in the introduction section along with an overview of this technology. The second section presents the requirements that apply to civil aviation with an emphasis on integrity, which is related to the safety of each operation. The third section breaks down the elements of GBAS in more detail, shows the flow of the most important equations for calculating protection levels (PLs), and highlights the impact of the ionosphere. Additionally, the third section clarifies the strategy developed for GBAS to deal with anomalous ionospheric spatial decorrelation and the role of the so-called ionospheric threat model. The fourth section summarizes and clarifies the published work related to GBAS in Brazil, focusing on the most relevant conclusions that have supported decisions by Brazilian authorities. The fifth section discusses the most promising aspects for future GBAS architectures, i.e., the use of dual-frequency and multiconstellation. The final section summarizes and concludes the paper.

PERFORMANCE AND SAFETY REQUIREMENTS

All civil aviation requirements relevant to the scope of this paper are based on four key performance parameters, namely: accuracy, integrity, continuity, and availability. These parameters must be considered for any means of navigation, independent of the system employed to achieve them. Navigation system performance requirements are defined in Doc 9613, performance-based navigation (PBN) manual (ICAO 2014) for categories of procedures known as area navigation (RNAV) and required navigation performance (RNP). When used for approach procedures, these are classified as NPAs. Additionally, the standard and recommended practices (SARPs) of the International Civil Aviation Organization (ICAO) annex 10 presents all the requirements considering the following definitions (ICAO 2020b):

- Accuracy: quantitative parameter that reflects the level of agreement between the estimated and the true position. Accuracy is always associated with a given confidence level which will express the probability that the estimated position contains the true one.
- Integrity: a trust measure regarding the correctness of the information supplied by the total system. The integrity requirement is met if a system can provide valid alerts (warnings) within a specified tolerance time when the estimated navigation errors exceed the thresholds for the intended operation.
- Continuity: capability of the system to perform its function without unscheduled interruptions during the intended operation. It can be interpreted as the probability that the system supports accuracy and integrity requirements throughout a flight operation without interruption;
- Availability: the portion of time the system is to be used for navigation and the accuracy, integrity, and continuity requirements are met.

Figure 1 illustrates these definitions in a simple way. The center of the circles is the estimated position determined by the aircraft navigation system(s). The blue dot is the true position. The difference between the estimated position and the true position is the true position error (PE) and represents the accuracy of the system at this moment in time ("epoch"). In reality, the true position of the aircraft, and, consequently, its actual PE are not known in real time. Hence, the system manufacturer must demonstrate the accuracy achieved by the system over time (i.e., over thousands of epochs) as part of a thorough certification process which will take into account analysis, simulation, test results, assumptions (if needed), and engineering arguments.
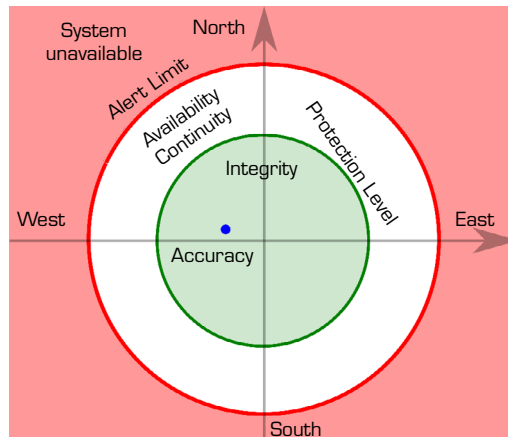

Source: Based on Lee (2005).

Figure 1. Navigation system performance requirements.

The inner circle in Fig. 1 represents a bound on the aircraft position error in a given direction. It is called the PL and is calculated in real time. Bounding error means that PLs must exceed the actual (unknown) error with a very small probability of failing to bound (e.g., less than 1 in 10^7, depending on the integrity requirements for a given application). The outer circle is the safe error threshold (tolerance) for a specific operation and is called the alert limit (AL). Alert limits are upper tolerable limits for the PLs, as they represent maximum "safe" navigation sensor error (NSE) above which the risk of an accident becomes too great. Therefore, once one or more calculated PLs exceed their ALs, the aircraft can no longer use GBAS for the current operation and must use different sensors or abort the operation.

For GBAS Category (CAT) I precision approaches, the AL values vary according to the distance to the runway threshold and have the minimum value of 10 m for the vertical component at the minimum decision height (DH) of 200 ft, which is where the pilot must decide whether or not to proceed with the approach based on visual conditions. A GBAS-supported operation is considered "available" as long as the PL is below the AL for each relevant position axis. If the PL exceeds the AL in one or more axes, the system is declared "unavailable", as long as this occurs before an aircraft begins an operation. If an aircraft has begun its operation and PL exceeds AL (after previously being below it), loss of continuity occurs, meaning that an abort is required unexpectedly.

Integrity is maintained when the true position is within the PL bounds, i.e., PE remains below PL, which also remains below AL, in each position axis. Loss of integrity occurs if no alert is issued (or corrective action is applied, such as excluding a faulty satellite) while the position error exceeds AL for a time longer than the specified time-to-alert (TTA). Figure 2 illustrates this with an example of six different situations (time slots) involving variations between PE and PL and their relation to AL from an integrity point of view.

Bin I in Fig. 2 (the left-hand column) represents nominal operation since PE is below PL and they are both below AL. In bins II and III, the system is unavailable because the PL is above the threshold. However, bin II was unnecessarily conservative since the PE is below the AL (keep in mind that PE is unknown in real time). The fourth and sixth bins depict the undesirable situation where PE is above the estimated PL, meaning that the estimated error bound does not cover the true error. In both of these bins, the navigation system can be classified as providing "misleading information", but the situation does not represent loss of integrity since both PE and PL are below AL in bin IV and above AL in bin VI. Bin V depicts the most critical situation because the PL is below AL, which allows the system to be used, but PE exceeds AL. If the situation in bin V occurs and the system does not remove the flawed measurements (so that PE falls back below AL) or notify the pilot within the specified TTA, loss of integrity occurs. In summary, integrity is lost when PLs in all monitored position axes are below the ALs in those axes, while the true position (unknown in real time) in any of those axes is greater than the AL for that axis.
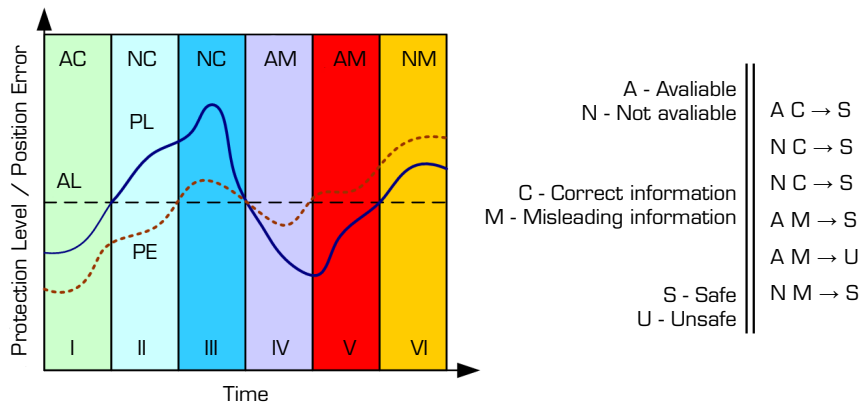
Source: Adapted from Hofmann-Wellenhof *et al.* (2008).

Figure 2. Protection level (PL) and position error (PE) from an integrity perspective.

Integrity loss is the most concerning issue for a navigation system, since it is directly safety related. In most cases, integrity cannot be measured in real-time. Previous (offline) studies and tests must determine the integrity of a navigation system in order to demonstrate that the probability of loss of integrity is below the requirement specified for the desired operation.

Table 1, with information extracted from ICAO Annex 10 (ICAO 2020b), presents the performance requirements for different kinds of navigation procedures supported by GNSS. Non-precision approach based on GNSS uses vertical guidance from the barometric altimeter and 2D horizontal positioning from GNSS. Approach procedure with vertical guidance I (APV-I) and approach procedure with vertical guidance II (APV-II), shown in Table 1, are also known as localizer performance with vertical guidance (LPV) and have more stringent requirements than NPA because they also provide vertical navigation from GNSS. Currently, APV and LPV are typically performed using an SBAS covering the area where the operation takes place. Categories I, II and II (CAT I, CAT II, and CAT III) refer to the category of the approach procedure and the impaired visibility conditions that they are meant to overcome. They are considered PAs whose services are traditionally provided by ILS. Precision approaches provided by GNSS-based systems require augmentation of the satellite observations due to the demanding requirements shown for them in Table 1.

As expected, Table 1 shows that the more demanding the approach procedure, the more stringent are the performance requirements. Additionally, an interesting aspect to point out on the information shown in the table is that the integrity requirement is given in terms of the probability of loss of integrity (Pr[LoI]).

Table 1. Air navigation performance requirements.

Approach type	Accuracy (95% error)		Integrity		Alert limit		Continuity	Availability
	H (m)	V (m)	Time to alert (s)	Pr(LoI)	H (m)	V (m)		
NPA	220.0	-	10	1.10^{-7} / h	556.0	-	1.10^{-4} / h to 1.10^{-8} / h	0.99 to 0.99999
APV-I	16.0	20	10	2.10^{-7} / approach	40.0	50.0	8.10^{-6} per 15 s	0.99 to 0.99999
APV-II	16.0	8	6	2.10^{-7} / approach	40.0	20.0	8.10^{-6} per 15 s	0.99 to 0.99999
CAT I	16.0	4	6	2.10^{-7} / approach	40.0	10.0	8.10^{-6} per 15 s	0.99 to 0.99999
CAT II	6.9	2	2	2.10^{-9} / approach	17.4	5.3	4.10^{-6} per 15 s	0.99 to 0.99999
CAT III	6.1	2	1	2.10^{-9} / approach	15.5	5.3	2.10^{-6} per 15 s	0.99 to 0.99999

Source: ICAO (2020b). NPA: Non-precision approach; APV: Approach procedure with vertical guidance; CAT: Category; H: Horizontal; V: Vertical; Pr(LoI): Probability of loss of integrity.

The Ground-Based Augmentation System
System overview

Ground-Based Augmentation System was designed to support precision approaches, with the additional possibility of supporting GNSS-based navigation in the terminal area of equipped airports within a maximum use distance of 23 nautical miles from the facility (RTCA 2017). In GBAS terminology, a GBAS facility that supports CAT I provides GBAS approach service type C (GAST-C). The GBAS approach service type D (GAST-D) supports CAT II and CAT III approaches as well as CAT I approaches based upon additional requirements on airborne equipage and ground-aircraft interaction, as will be explained below. Future GAST-E and -F versions of GBAS are expected to support all these operations without many of the additional requirements of GAST-D.

The operational principle of GBAS is the same as that of differential GPS (D-GPS), in which a stationary ground receiver in a surveyed location, viewing the same satellites as the user, provides differential corrections that, when applied by users, remove range errors that are common to both ground receiver and user. This reduces user position estimation errors and thus improves accuracy (Hofmann-Wellenhof *et al.* 2008).

Each GBAS facility broadcasts pseudorange corrections for each satellite (type 1 messages) on the VHF band used by ILS localizers (108–118 MHz) to aircraft along with integrity parameters (type 2 messages) and the approach paths to the airport supported by that facility (type 4 messages). These VHF transmissions make up what is known as the VHF data broadcast (VDB). Precision approaches are executed by aircraft equipped with GPS receivers and modified ILS localizer receivers designed to decode the VDB messages broadcast by the ground facility.

The ground station calculates corrections for each visible and usable satellite for L1 code pseudorange measurements only. The GPS L2 frequency is not employed by civil aircraft because it is not in an aeronautical radionavigation service (ARNS) band and thus cannot be protected from interference by civil aviation service providers.

With a single frequency receiver, it is not possible to directly measure the absolute delay caused by the ionosphere. However, the GPS block IIF and block III satellites also broadcast signals at the L5 frequency for civilian applications (1,176.45 MHz). Using both L1 and L5 frequencies, it is possible to obtain ionosphere-free range measurements that would minimize the residual (higher-order) ionospheric error (Felux *et al.* 2017a). For example, Tang *et al.* (2009) performed positioning tests using L1 and L2 on airborne receivers, with L2 substituting for L5 before the L5 frequency was available from many satellites. The results showed improvements in positioning, however, with a high level of noise on L2 due to the use of semi-codeless L2 measurements.

While versions of GBAS that make use of both L1 and L5 measurements are under development, the current GBAS architecture provides corrections only for code pseudorange measurements on L1. Figure 3 illustrates, in a simplified way, the overall information flow of a GBAS facility and nearby aircraft. In summary, both the airborne and the ground receivers track the locally-visible GPS satellites and measure their L1 C/A-code pseudoranges. The ground facility computes pseudorange corrections for each satellite and broadcasts messages with these corrections along with additional integrity-related parameters. The presence of a correction for a given satellite is one "integrity parameter", as satellites that are visible to nearby aircraft but which do not have corrections provided for them do not have assured integrity and thus are not included in aircraft position calculations.

From its measured pseudoranges and the corrections and other parameters received from the ground station, the aircraft navigation system applies the corrections for each satellite it has a measurement for, computes its position from the set of satellites with ground corrections and valid airborne measurements, and estimates error bounds on this position. If these protection levels do not exceed predefined thresholds (ALs), the aircraft performs the selected approach procedure using the approach path geometry broadcast from the ground station.

The ground facility obtains the corrections broadcast in type 1 messages by comparing the predicted pseudorange with the measured pseudorange for each tracked satellite. Figure 4 depicts the elements included in the correction calculations. The position of the reference receiver antennas within the ground facility are well known since they were previously surveyed to centimeter-level accuracy. Using the coordinates of these antennas, vector R is determined from the origin of the coordinate system (mass center of the Earth). The theoretical orbit path for each satellite is known from the navigation messages broadcast by the satellites, allowing the vector S to be determined at each epoch. From vectors R and S, vectors defining the separations between the ground antennas and satellites (PR_{SR}) can be easily obtained for current and future epochs. The corrections for each satellite will be the difference between calculated and measured pseudoranges, where the measured pseudoranges are the outputs of first-order carrier smoothing filters with time constants of 100 s (RTCA 2017).
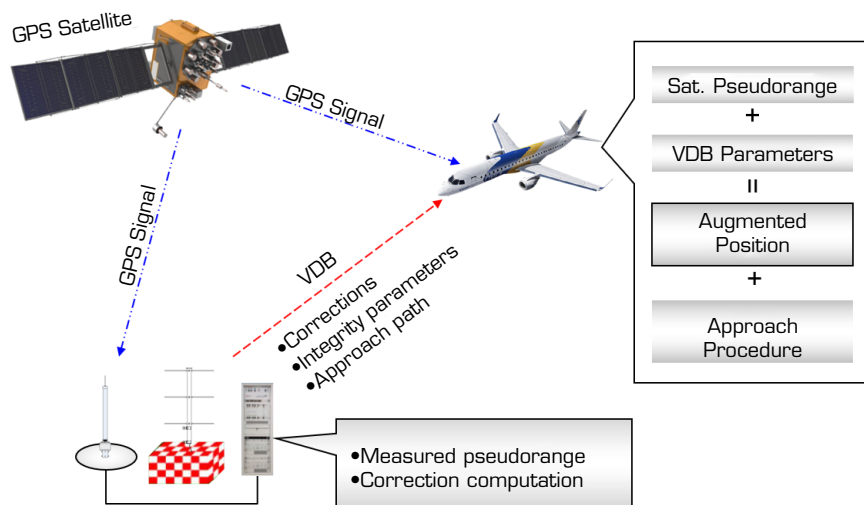
Source: Developed by the authors.

Figure 3. Ground-Based Augmentation System information workflow.
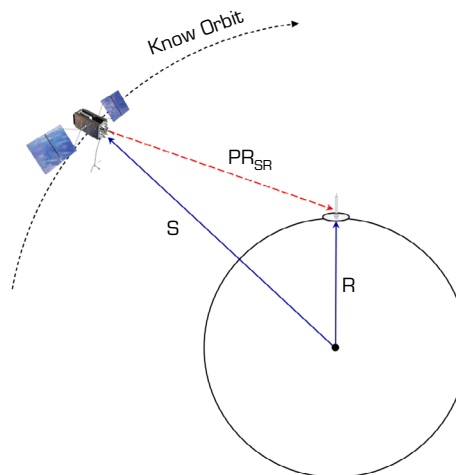
Source: Developed by the authors.

**Figure 4.** Elements involved in the pseudorange correction of a GBAS.

The equations related to the correction calculation are detailed in DO-245A (RTCA 2004). The smoothing filter is presented in Section 3.2.5.1.1 of DO-245A, as well as Section 3.6.5.1 of ICAO (2020b). The pseudorange correction for each satellite is formed by averaging among the candidate pseudorange corrections generated by each reference receiver. One complication is that each reference receiver has a different clock bias term, and these are also different than the airborne receiver clock bias. Therefore, an estimate of each reference receiver clock bias is derived and removed from that receiver's candidate pseudorange correction before these corrections are averaged into a single correction for each satellite and sent to aircraft. The equations for the clock adjustment and the final calculation of the averaged corrections for each satellite are shown in Appendix E, Section E3 of DO-245A.

Along with the corrections in type 1 messages, GBAS also transmits integrity-related parameters in type 2 messages. These are used by the airborne system to compute lateral (1D cross-track), horizontal (2D), and vertical protection levels (LPL, HPL, and VPL, respectively). The latter is the most critical since the vertical component of GPS positioning is typically worse than the two horizontal components due to the properties of GPS satellite geometries as viewed from the earth.

Ground-Based Augmentation System has redundancy at multiple points in order to maintain integrity, as well as availability and continuity. For example, four separate reference receivers and antennas are used to mitigate possible faults in these receivers. Differential corrections are calculated for each reference receiver, and the average among them is normally broadcast. If one of the receivers computes a correction for a particular satellite that is significantly different from the mean of the corrections of the other receivers, that measurement is dropped from the calculation. If measurements from one receiver are discarded such that fewer than four satellites are approved from it, it is excluded from use. The system still can operate normally with the three remaining receivers (protecting availability), but a maintenance alert is issued. If two of four receivers are excluded, no new precision approaches can begin, but the ones already begun can be completed (to maintain continuity). Exclusion of more than two of the four reference receivers/antennas combinations is one of the (rare) conditions under which a GBAS facility becomes completely unusable (e.g., it broadcasts type 1 messages with no valid corrections).

Each GBAS ground facility has a series of monitors to check for consistency of the measurements between the reference receivers, the evolution of the measurements in time, possible distortions in the received signals, satellite clock and ephemeris errors etc. These monitors are meant to detect all threatening errors due to satellite anomalies as well as detecting faulty reference receiver measurements prior to the calculation of corrections. The development of these monitors as part of the Stanford GBAS integrity monitor testbed (IMT) is described in Xie (2003). More information regarding the concepts behind these monitors and the information flow between them are in Pullen and Enge (2007) and Pullen (2017).

In addition, GBAS transmits type 4 messages that contain information about the approach procedures supported by a GBAS-equipped airport. This message usually contains several data sets to support different procedures for multiple runway ends, each of which has a separate reference path designator and identifier. Note that a single runway end can have multiple landing procedures, including variations on the touchdown point and the glide path angle. This type of message also transmits the ALs (horizontal and vertical), which are safety tolerances that the protection levels must remain within. The relationship between the PLs computed onboard aircraft and these ALs in nominal operation is illustrated in Fig. 5. Note that, as previously illustrated in Fig.1, if a PL exceeds the AL for a particular operation, then the system will be unavailable for that particular operation. If an operation is already underway when PL grows to exceed AL, that operation would be aborted in favor of a safer backup mode of flight.

Alert Limit
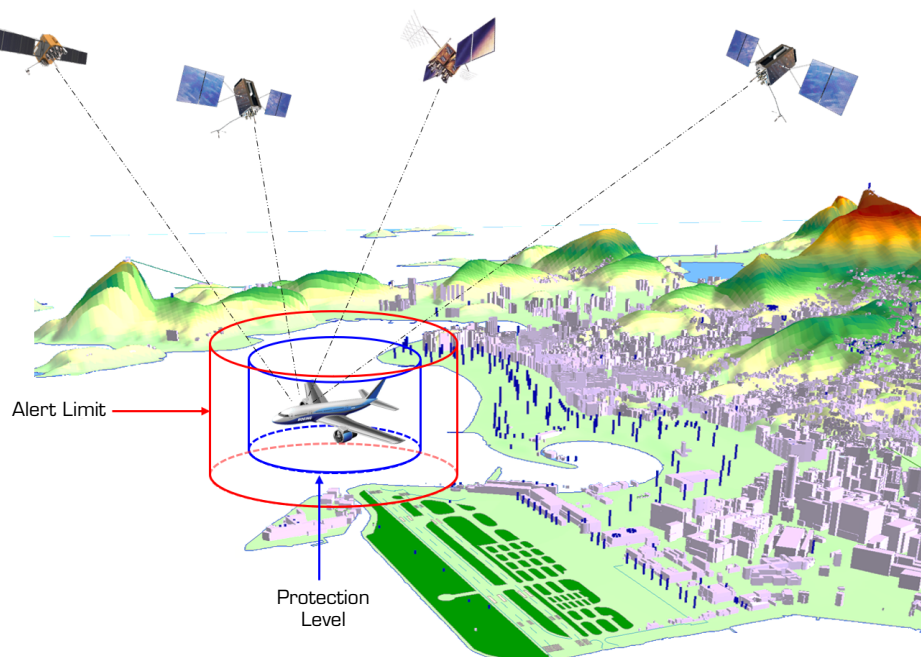
Protection Level

Source: Developed by the authors.

Figure 5. Relationship between AL and PLs in nominal operation.

Vertical protection level computation

The calculation of PLs is an error propagation process that takes into account many variables, models, and parameters transmitted by the GBAS ground facility. The details of these calculations were standardized by Special Committee 159 of the Radio Technical Commission for Aeronautics (RTCA) in the document *Minimum Operational Performance Standards for GPS/Local Area Augmentation System Airborne Equipment*, DO-253D in the most recent revision (RTCA 2017).

The vertical direction requirement is more stringent than the lateral direction, and vertical errors are almost always larger than lateral errors (all else being equal). While this paper will focus on VPL, the calculations for LPL are almost completely analogous. In GBAS, three different VPLs are computed to represent three different error state hypotheses: H_e represents an ephemeris fault on a single satellite (VPL_e); H_1 represents fault on a single reference receiver (VPL_{H1}); and H_0 represents nominal conditions with no faults or anomalies present (VPL_{H0}). In this paper, only the computation under the "fault-free" hypothesis will be presented. The equations for all hypotheses can be found in RTCA (2017).

The main aspects of the VPL computation are presented backwards for the sake of better understanding. This means they will not be presented in the order they are computed, but, instead, the general VPL equation will be presented first and broken down into its main elements. Since VPL is intended to bound low-probability vertical positioning error (VPE), its calculation is directly related to the estimation of VPE. Assuming that vertical position errors under nominal conditions are Gaussian distributed with a mean of zero, VPL is given by Eq. 1 (RTCA 2017):

$$VPL = K_{ffmd}\, \sigma_{VPE} + D_V \tag{1}$$

where, σ_{VPE} is the bounding standard deviation of the vertical component of the positioning error (see Eq. 2); K_{ffmd} is the multiplier (unitless) which extrapolates the bounding error standard deviation to the sub-allocated integrity probability required for the H_0 hypothesis (given by P_{ffmd}). The allocation that generates P_{ffmd} is dependent on the number of reference receivers used by the ground system to compute differential corrections. D_V is a GAST-D specific term (which is set to zero for GAST-C) that represents the magnitude of the difference between vertical position solutions derived from 30 and 100 s smoothed pseudoranges.

The standard deviation of the vertical positioning error is an error propagation of the N satellite pseudoranges that were used in the navigation solution. Assuming the measurement errors from different satellites to be zero-mean, uncorrelated, and Gaussian distributed, the vertical positioning error standard deviation is computed as (RTCA 2017):

$$\sigma_{VPE} = \sqrt{\sum_{n=1}^{N} S_{vertical,n}^2 \cdot \sigma_{PR,n}^2} \tag{2}$$

where, $S_{vertical,n}^2$ is the vertical projection factor in the along-track (positive forward)/cross-track (positive left)/up coordinate system (note that "cross-track" corresponds to the lateral dimension); $\sigma_{PR,n}$ is the standard deviation of the error in the corrected pseudorange measurement for the nth satellite.

For each pseudorange measurement, the error model takes into account four different (and assumed to be uncorrelated) errors and is given by:

$$\sigma_{PR_n} = \sqrt{\sigma_{air_n}^2 + \sigma_{tropo_n}^2 + \sigma_{iono_n}^2 + \sigma_{pr\_gnd_n}^2} \tag{3}$$

where, σ_{air_n} is the airborne error determined from the receiver noise estimate and a specified multipath model; σ_{tropo_n} is the standard deviation of the error in the tropospheric correction; σ_{iono_n} is the residual ionospheric uncertainty error; $\sigma_{pr\_gnd_n}$ is the ground system error that includes ground station receiver noise and multipath error and is broadcast in type 2 messages.

All of the above pseudorange error components have specific models. These models, when combined to generate σ_{PR_n} in Eq. 3, are meant to conservatively bound the standard deviation of pseudorange error such that the extrapolation of the position error standard deviation σ_{VPE} from Eq. 2 to the very low probability protected by VPL$_{H0}$ in Eq. 1 remains a bound—in other words, the probability of the actual VPE exceeding VPL$_{H0}$ is no greater than P_{ffmd}. Note that, while standard models for $\sigma_{pr\_gnd_n}$ exist (e.g., see RTCA 2004), they are not guaranteed to sufficiently bound actual errors for every ground station installation, so this must be validated with specialized analysis and data (Blanch *et al.* 2019; Larson *et al.* 2019).

Due to the impact of the ionosphere on system performance, only σ_{iono} will be explored in further detail. Its calculation considers a one-sigma bounding value for typical ionospheric gradients (including those under active conditions) and the "memory" of past measurements within the carrier smoothing filter applied to pseudorange measurements. σ_{iono} is computed as (RTCA 2017):

$$\sigma_{iono(i)} = F_{pp} . \sigma_{vig} . (X_{air} + 2.\tau.v_{air}) \tag{4}$$

where, F_{pp} is the obliquity factor to convert from vertical measurements to slant for a given satellite, calculated by:

$$F_{pp} = \left[1 - \left(\frac{R_e cos(el_n)}{R_e + h_I} \right)^2 \right]^{-\frac{1}{2}} \tag{5}$$

where, R_e is the mean radius of the Earth = 6,378.136 km; h_1 is the mean height of the ionosphere considering the thin shell model (typically taken to be 350 km); el_n is the elevation angle of the nth satellite; σ_{vig} bounding standard deviation of a zero-mean Gaussian distribution describing zenith ionospheric gradients due to spatial decorrelation between the reference station and the aircraft; X_{air} is the 2D horizontal distance between the aircraft and the GBAS reference point; τ is the time constant of the code smoothing filter (typically 100 s); v_{air} is the horizontal speed of the aircraft.

A detailed derivation of Eq. 4 is given in Ko (2000). The value of σ_{vig} is broadcast in the type 2 message and must be previously determined by data analysis for each region like the ones performed by Lee *et al.* (2007) for the CONUS and by Chang *et al.* (2019; 2021) for Brazil. This value, when extrapolated to the very low probability represented by P_{ffmd} (e.g., 5 × 10^{-9} for M = 4 reference receivers), needs to bound both quiet and active ionospheric conditions in the region where GBAS is fielded, but not rare, anomalous conditions. These are treated as threats and are handled differently, as described in the following sections.

Ionospheric threat model and GBAS mitigation

Different types of errors affect GNSS performance, but, among them, errors caused by the ionosphere are the most significant due to their unpredictability. For air navigation applications, unusual ionospheric errors become critical integrity and continuity issues during the more demanding phases of flight, such as precision approach and landing, due to the importance of vertical position estimates and the low error tolerances on these estimates (i.e., low ALs).

A detailed review of the characteristics and dynamics of low-latitude ionosphere is presented in the follow-on paper of this two-part series. Briefly, the ionosphere causes refraction in GNSS signals, changing their speed of propagation and resulting in deviations in user range measurements (equal delays in code measurements and advances in phase measurements) from what they would be if the ionosphere were not present.

The ionospheric impact on GBAS is caused mostly by spatial decorrelation. As previously depicted in Fig. 3, GBAS provides pseudorange corrections based on the lines of sight between the ground antennas and each satellite in view. The lines of sight between the airborne receiver and the same satellites are very similar to those from the ground station, but they are not the same. For the airborne receiver, the corrections received from the ground station will be more and more uncorrelated the longer the distance between the aircraft and the ground station.

Ionosphere behavior can be significantly different in the lines of sight from the ground station and the aircraft to the same satellite, as illustrated in Fig. 6. In this case, a difference in ionospheric total electron content (TEC) causes the delay experienced by the ground facility to differ from the delay experienced by the aircraft. The gradient in ionospheric TEC over the horizontal separation between ground facility and aircraft is represented by the σ_{vig} parameter included in Eq. 4.
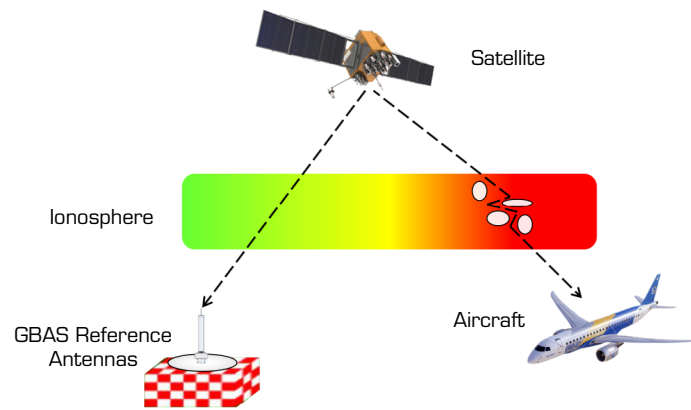
Source: Developed by the authors.

Figure 6. Spatial decorrelation between aircraft and GBAS ground station.

As part of GBAS safety assessment, it is a common practice to find the worst possible slant ionospheric gradient on the regions the system will be deployed. This parameter comes from studies of observed ionospheric behaviors to determine how large these gradients can be. The results of these studies for a specific region (plus margin for residual uncertainty) are used to establish the ionospheric threat model for that region. The first GBAS ionospheric threat models assumed that the maximum gradients were dependent on satellite elevation angle. However, it is currently believed that the highest gradient found in a specific elevation angle for a satellite can occur at any elevation angle.

Since the ground station has no real-time knowledge of the ionosphere affecting the line of sight between the aircraft and the satellites, situations can occur when the value of σ_{vig} is not large enough to bound the residual ionospheric errors within the nominal protection level (VPL_{H0}). When anomalous ionospheric gradients occur that are not bounded by a Gaussian ($0, \sigma_{vig}$) distribution, a different strategy must be used. The most common approach is called geometry screening and is applied in the position domain (Lee *et al*. 2011). Rather than treating gradients as randomly distributed, geometry screening assumes that the worst gradient within a constrained ionospheric threat model is always present in the worst possible configuration, as depicted in Fig. 7.
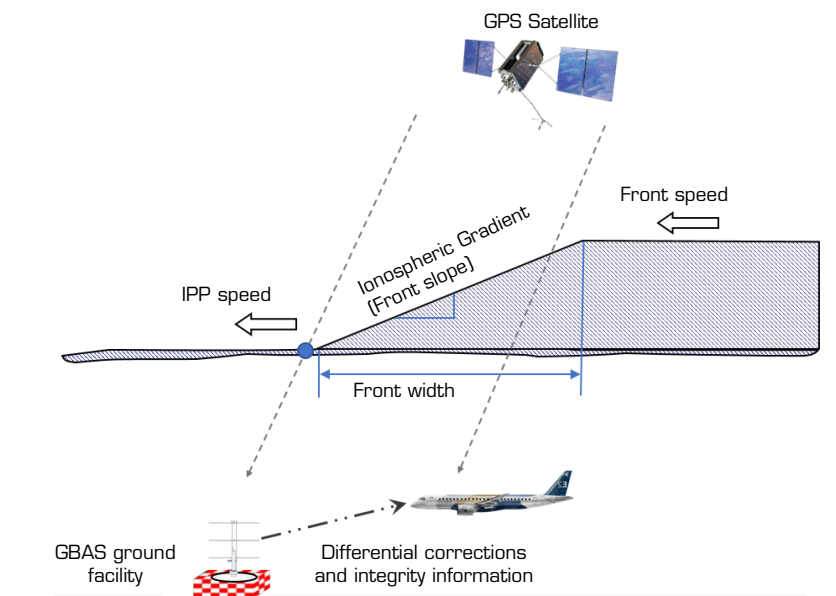
Source: Based on Lee *et al.* (2011).

Figure 7. Threatening configuration among the GBAS ground facility, the aircraft, and an ionospheric front with a large gradient.

Figure 7 shows the ionospheric pierce point (IPP) for a line of sight between the ground station and a specific satellite passing through a region of the ionosphere with a relatively low value for the TEC, which represents the ion density of the ionosphere. Also, the line of sight between the same satellite and the aircraft is shown crossing a higher TEC region. The differential corrections received by the aircraft would not be enough to mitigate the errors caused by the ionosphere in this case, since they were computed under significantly different conditions. Figure 7 also shows that the ionospheric TEC gradient is moving with respect to the ground, characterizing an ionospheric front that, in this case, has the same speed and direction as the IPP motion caused by satellite motion in its orbit. That is the most critical configuration because, if the velocity of the front is significantly higher or lower or if the alignment of the front is different, the ground station will observe a large ionospheric rate of change with time and would detect and exclude the affected satellite using the code-carrier divergence (CCD) monitor within the GBAS ground station. If ionospheric front motion is "masked" by similar IPP motion, no significant rate of change is present for CCD to observe, which could lead to large unmitigated error on the affected satellite(s) and thus loss of integrity.

Datta-Barua *et al.* (2010) present the detailed threat model parametrization and the results found for the CONUS. The worst gradients were found at the occasion of a strong magnetic storm, with disturbance storm-time (Dst) index in the order of –470 occurred in October and November 2003 and resulted in slant gradients on the order of 400 mm·km^{-1}, front width varying from 25 to 200 km and speeds up to 750 m·s^{-1}. Mayer *et al.* (2009) developed an ionospheric threat model for Germany and found the highest gradients to be below 200 mm·km^{-1}, similar widths found in CONUS and speeds reaching up to 1200 m·s^{-1}. Later, Robert *et al.* (2018) developed an ionospheric threat model for the whole Europe (including peripheral regions influenced by equatorial ionospheric behavior) and found the highest gradients to be on the order of 400 mm·km^{-1}.

Based on the scenario described above, geometry screening computes the vertical error of the aircraft induced by the worst possible ionospheric gradient, simultaneously affecting two satellites. This value is known as the maximum ionosphere-induced error in vertical (MIEV). A separate MIEV calculation is performed for each subset of GBAS-approved satellites that aircraft could be using for positioning (e.g., all approved satellites, all minus any one satellite, and all minus any two satellites) and is based on the aircraft having reached the CAT I minimum decision height of 200 ft, which is typically the most constraining case. Each MIEV is compared to the tolerable error limit (TEL) at this point on the approach, which is 28.8 m and was derived by the CAT I approach safety assessment in Shively and Niles (2008). The worst slant gradient used in the calculation of the MIEVs comes from the ionospheric threat model derived for the region of interest.

After computing worst-case vertical errors (MIEVs) for each subset satellite geometry and the DH location of each runway end supported by CAT I GBAS, geometry screening checks if any of these MIEVs exceed TEL. If yes, then the algorithm checks each of these cases to see if the VPL computed for any of them with the nominal σ_{vig} is above the vertical AL (VAL), meaning that aircraft would be allowed to begin approaches under these conditions. To prevent this, if VPL is below VAL for cases where MIEV is above TEL, σ_{vig} (or other broadcast parameters) must be inflated until VPL is above VAL, making these cases (subset geometries and/or runway ends) unavailable and, thus, unusable. This roundabout procedure is required because aircraft using CAT I GBAS do not know about TEL and cannot compute MIEV; thus, they need to be warned of situations where MIEV exceeds TEL in terms of VPL (which they compute based on ground inputs) and VAL.

Figure 8 illustrates an example of ground screening presented by Lee *et al.* (2011) in which MIEV was computed for all possible subset satellite geometries at a particular place (Newark, NJ, USA) and time of day. A single approach direction and distance of 6 km between DH and ground system locations was assumed, and 29 different satellite geometry indices are shown on the x-axis, where index 1 represents the all-in-view geometry and the remainder represent subsets of it. For all but subset indices 4, 17, and 25, nominal and inflated VPLs appear (compared to VAL) along with MIEV (compared to TEL). No VPLs or MIEVs are shown for subsets 4, 17, and 25 because their uninflated VPLs exceed VAL without inflation, making them unavailable and, thus, nonthreatening by definition. Eight of the other subsets (6, 7, 11, 12, 16, 21, 24, and 26) have MIEV > TEL, and thus require parameter inflation. Just enough σ_{vig} inflation is applied to make the VPLs for all eight of these subsets slightly exceed VAL so that they become unusable and nonthreatening as well.
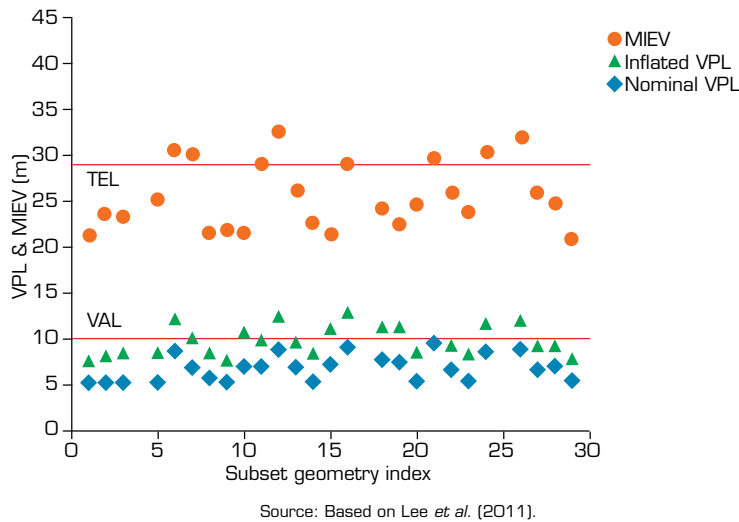
Source: Based on Lee *et al.* (2011).

**Figure 8.** Effects of σ_{vig} inflation on VPL and removal of MIEV > TEL cases.

Geometry screening based on inflation of σ_{vig} is painful because it significantly reduces CAT I GBAS availability below what it would be if threatening ionospheric gradients could not occur. This happens because the σ_{vig} inflation needed to increase the VPL of threatening geometries (and make them unavailable) also affects non-threatening geometries and makes some of them unavailable as well. This can be seen in Fig. 8, where geometry indices 10, 15, 18 and 19 have MIEV below TEL and uninflated VPL below VAL, but VAL increases above VAL when inflation is applied to protect other subset geometries. Because the availability loss due to geometry screening is a limiting factor for CAT I GBAS (Pullen *et al.* 2010), other inflation techniques that modify other integrity-related parameters, such as σ_{pr_gnd} and the ephemeris p-values, have also been examined (Ramakrishnan *et al.* 2008; Seo *et al.* 2012).

Ground-based augmentation system approach service type D (GAST-D)

Ground-based augmentation system approach service type D (GAST-D) is a relatively new GBAS service type that supports CAT II/III precision approaches and landings based upon ground-system and aircraft upgrades and new integrity monitor requirements in both places. As explained above, CAT I (GAST-C) GBAS broadcasts corrections based on ground receiver pseudorange measurements that are smoothed by carrier-phase measurements over a time constant τ using the methodology first proposed by Hatch (1982). Longer time constants have the effect of further reducing ground system errors, particularly those with correlation times shorter than the selected time constant. For this reason, a relatively long time constant of 100 s is used in both ground and airborne receivers for GAST-C. One of the main modifications in GAST-D is shortening the time constant of the ground and airborne smoothing filters that produce pseudoranges for navigation to 30 s (RTCA 2017). This reduced filter time constant makes the outputs noisier and more sensitive to sudden variations, but this is outweighed by the reduction in differential ionospheric error under nominal and threatening conditions shown in Eq. 4.

In GAST-C, the ground station has the entire responsibility for ionospheric threat mitigation, and the resulting mitigation methods (such as geometry screening) must make conservative assumptions. However, in GAST-D, both ground and airborne subsystems share this responsibility (Pullen *et al.* 2017). The combination of ground and airborne observability of rapid ionospheric changes helps reduce the scope of uncertainty in real-time ionospheric behavior and reduce conservatism.

Pullen *et al.* (2017) present the main requirements for GAST-D in terms of ionospheric threat mitigation. In GAST-D, the ground station implements an ionospheric gradient monitor (IGM) in addition to the CCD monitor already used in GAST-C. Ionospheric gradient monitor is required to detect all gradients that are affecting one or more ground system reference receivers, even if the rate of change of ionospheric delay over time is nominal. This requires that the reference receiver antennas be separated by at least several hundred meters and be oriented such that gradients affecting each approach direction are observable to at least one pair of these antennas (Belabbas *et al.* 2011; Khanafseh *et al.* 2012). Figure 9 shows an example of a rectangular box orientation of reference receiver antennas for a GAST-D facility with antenna separation distances identified as *a* and *b* (where *a* and *b* might be the same or different) (Reuter *et al.* 2012). Several analyses of possible receiver orientations and separation distances have been conducted (e.g., see Jing *et al.* 2015), mostly suggesting separations from 150 m to 1 km.
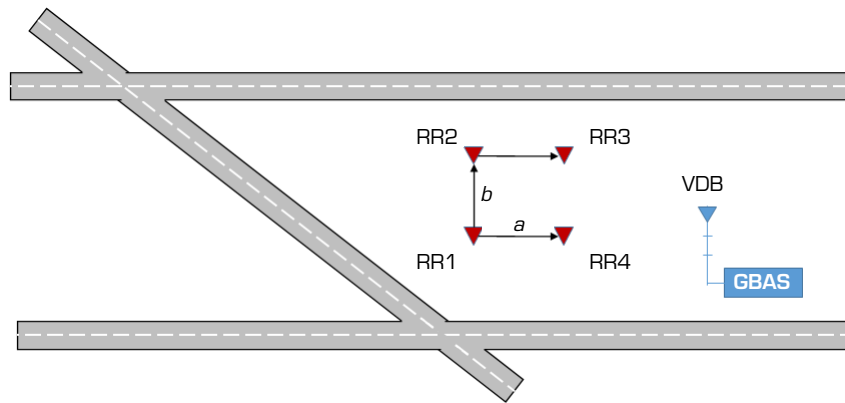
Source: Developed by the authors.

Figure 9. Example of reference receiver (RR) antenna orientation for a GAST-D facility.

On the airborne side, two additional monitors targeted at ionospheric threats are included when using GAST-D: the dual-solution ionospheric gradient monitoring architecture (DSIGMA) and an airborne CCD monitor similar to the one implemented on the ground (Pullen *et al.* 2017). The DSIGMA monitor compares two position solutions computed separately from the 100 and 30 s smoothed pseudoranges. If the absolute value of the difference between these two position solutions in the vertical or lateral direction exceeds 2 m, DSIGMA degrades the available approach service type to GAST-C. Note that, by design, GAST-D stations support GAST-C-only aircraft as well and thus can fall back to GAST-C service (for both GAST-C and GAST-D equipped aircraft) when ionospheric conditions require it.

In GAST-D, geometry screening is performed by the aircraft to limit the positions errors that may occur and cope with the stringent requirements of CAT III standards. Performing this task at the aircraft makes use of the known aircraft satellite geometry and avoids the conservatism implied by the ground system having to protect all possible subset geometries that might be used.

Regarding the monitors run in the airborne subsystem for GAST-D, Dautermann *et al.* (2012) present a detailed diagram of the airborne monitoring flow with each segment classified as a legacy GAST-C monitor or a new GAST-D monitor. In the diagram provided by the authors, each monitor is also referenced by the specific Minimum Operational Performance Standards (MOPS) subsection that describes each one for GAST-C (DO-253C, RTCA 2008) or GAST-D (DO-253D, RTCA 2017).

In short, GAST-D is an extension of GAST-C scheme with additional detection logic and more sensitive monitors to meet the stringent performance requirements for CAT II/III (Murphy *et al.* 2012). It has not been fully tested in low latitudes in the presence of equatorial plasma bubbles. Saito *et al.* (2015) performed some tests of IGM in a low-latitude environment in Japan but, curiously, the anomalous behaviors found were due to small-scale tropospheric delay gradients caused by local atmospheric heating. These events are normally too small to notice but are large enough to violate the very tight gradient thresholds of the IGM.

Due to the high sensitivity of the required monitors and the strong ionospheric dynamics in low latitudes, it is speculated that a GAST-D facility in Brazil would result in lower-than-feasible service availability. The challenges posed by ionospheric behavior to GBAS service in Brazil are described in the next section.

GROUND-BASED AUGMENTATION SYSTEM IN BRAZIL

As explained above with respect to geometry screening, the definition of the ionospheric threat model for the region of operation is vitally important. In Brazil, initial results of efforts to define a Brazilian ionospheric threat model were published by Lee *et al.* (2015) and Yoon *et al.* (2017a), which summarized the work of Mirus Technology (2015). A validation methodology for the highest gradients found in the Brazilian threat model is described in Yoon *et al.* (2015) and Yoon *et al.* (2017b). In all of these work, the same dataset was used: several South American reference station networks collected data from more than 120 ground stations spread across Brazil between the years 2011 and 2014, near and just after the peak of the previous solar maximum. More

than 100 days were chosen to be processed using the criteria of known occurrence of scintillation (S_4 index higher than 0.6), presence of geomagnetic storms (Kp exceeding 5 and Dst lower than –200), low ionospheric activity (as a control dataset), and other non-nominal days with some level of ionospheric disturbance.

The highest slant gradient found and validated in Brazil was around 850 mm·km^{-1} and was observed on GPS satellite from pseudorandom noise (PRN) 03 on March 1, 2014 at 01:14 Coordinated Universal Time (UTC) by a pair of stations located in São José dos Campos (in the southeastern region of Brazil) separated by about 9 km on a vector well-aligned with the geomagnetic equator (magnetic azimuth 289°). This gradient is twice as high as the highest gradient observed and validated in CONUS (on November 20, 2003). Regarding validation, a thorough analysis of this specific gradient of 850 mm·km^{-1} was performed by Yoon *et al.* (2020), which confirmed that it was caused by an ionospheric plasma bubble depletion as opposed to receiver measurement errors or cycle slips. The authors also confirmed that the same plasma bubble event triggered other very high gradients (above 400 mm·km^{-1}) on the same night.

Beyond this event, dozens of gradients exceeding the CONUS threat model bound were detected and validated in Brazil during the study period. Figure 10 shows two plots containing all the gradients for the Brazilian threat model. The left-handed panel of Fig. 10 depicts the distribution of gradients as a function of satellite elevation angle and shows the CONUS ionospheric threat model bound as a reference. The right-hand panel of Fig. 10 shows the distribution of gradients as a function of their time of occurrence in UTC. The vast majority of reference stations providing data are located in the time zone UTC-3. From Fig. 10b, it is clear that almost 100% of the gradients detected as part of the Brazilian ionospheric threat model occur during local nighttime in Brazil.

Translating the x-axis of Fig. 10b to local time in the Eastern time zone of Brazil, one can observe that the largest gradients found occurred between approximately 18:00 LT and 3:00 LT. That is strong evidence that these gradients were caused by plasma bubble events, as confirmed by Yoon *et al.* (2020). This behavior was expected since most of the processed days were chosen based on the occurrence of nighttime scintillation (Lee *et al.* 2015; Yoon *et al.* 2017a).
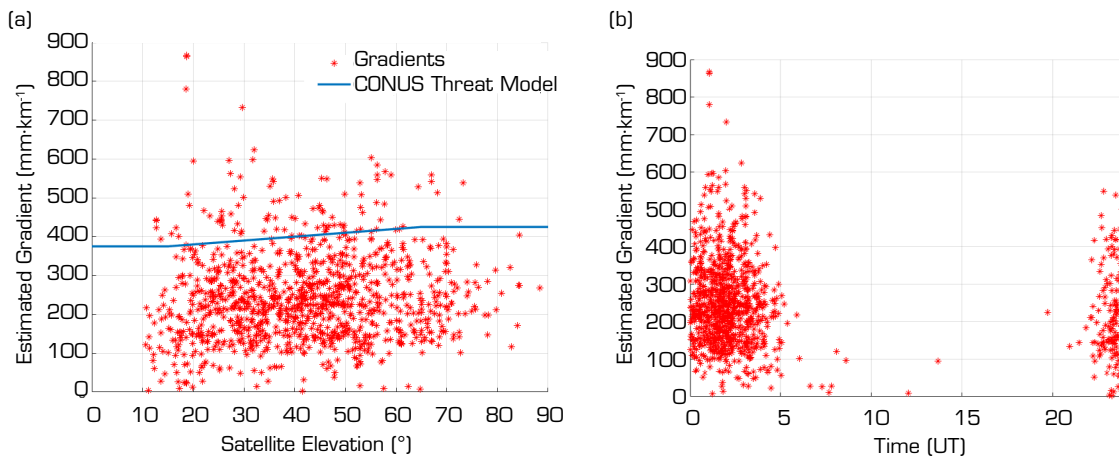
Source: Data from Mirus Technology (2015).

Figure 10. Observed gradients making up the Brazilian ionospheric threat model. (a) Distribution with respect to satellite elevation angle, CONUS threat model is shown as a reference; (b) Time distribution of gradients.

Using the geometry screening approach described in Lee *et al.* (2011) that assumes the highest gradient is always present in the worst configuration, Yoon *et al.* (2016) ran a simulation to assess GBAS performance in Rio de Janeiro international airport using different maximum gradient values. The authors considered the CONUS threat model to apply during daytime (with a maximum gradient of 425 mm·km^{-1}) and different (higher) maximum gradient values during nighttime. Using this time-dependent mixed threat model, the resulting availability was found to be 99.3% during daytime and only 58% during nighttime with the largest gradient tested.

The preliminary Brazilian threat model shown above provides important knowledge of how large threatening gradients can be in Brazil. With this in mind, the DECEA in Brazil has supported efforts to determine the conditions under which it is practical to

operate GBAS stations in the country. These efforts have led to three different lines of investigation under the assumption that no significant changes in the CAT I (GAST-C) GBAS architecture would be made: 1) determining the nominal σ_{vig} to be broadcast by the ground station; 2) determining the periods of the day when a GBAS station can operate safely with the current architecture; 3) determining if the existing CONUS threat model is suitable during the hours of operation established in step 2.

The results of these efforts can be found in Chang *et al.* (2019; 2021) and are summarized as follows. The nominal σ_{vig} was found to be 13 mm·km⁻¹, which, when combined via root sum square with the tropospheric gradient bound of 5 mm·km⁻¹ based on CONUS research (van Graas and Zhu 2011), rounds up to 14 mm·km⁻¹, which is the value that would be broadcast prior to any inflation based on geometry screening. The results determined that a GBAS station can safely operate with this (uninflated) value of σ_{vig} from approximately 06:00 to 18:00 h local time. Finally, it was verified from historical data that no threatening gradient exceeds the limits of the CONUS threat model when applied in Brazil during this definition of daytime.

The results of Chang *et al.* (2019; 2021), specifically regarding the hours of operation, impose a significant availability constraint for the use of GBAS in Brazil. This study assumed, for example, that anomalous ionospheric behavior would always occur during nighttime at any period of the year. Assuming the worst-case threat will always be present is a conservative approach that may be required to guarantee that the required levels of safety are met. One alternative is to separately monitor ionospheric gradients in real-time and broadcast integrity parameters according to the gradient conditions that they observe (as opposed to the worst possible conditions). A strategy along these lines has been proposed by Caamano *et al.* (2021) using a network of monitoring receivers around a GBAS facility in Alaska and a complex algorithm to detect and estimate ionospheric gradients in real-time. The proposed method shows satisfactory results using simulated gradients. However, its performance in low latitudes is uncertain and requires further analysis.

DUAL-FREQUENCY MULTI-CONSTELLATION GBAS

Given the poor performance of GBAS for GAST-C in Brazil, as demonstrated by the papers cited in the previous section, the expectations of the aviation community for GBAS in Brazil are focused on future dual frequency and multi-constellation approaches to GBAS.

As will be detailed in the subsequent paper, the main issue in low-latitude regions is the occurrence of equatorial plasma bubbles that can cause large and threatening gradients to GBAS. With a multi-constellation approach that includes Galileo and perhaps other GNSS satellites in addition to GBAS, it should be possible to conservatively detect and exclude satellites potentially affected by plasma bubbles while having enough remaining satellites to provide high accuracy and low protection levels. This concept has been applied by Caamano *et al.* (2016) to simulate the availability of a multi-constellation GBAS in a low-latitude region in the presence of one or more equatorial plasma bubbles. The simulated site was specifically Rio de Janeiro, and the constellations included were GPS and Galileo. The authors simulated different sizes of equatorial plasma bubbles occurring one at a time and also simultaneous occurrences of four to six plasma bubbles. The affected satellites were excluded, and the protection levels computed with the remaining satellites using the existing single-frequency approach. While the nominal σ_{vig} value was not included in the paper, nor was it made clear if geometry screening was applied, the authors found a significant improvement in the availability by using single-frequency GPS and Galileo as opposed to GPS alone. However, the issue of how to reliably detect affected satellites and thus mitigate plasma bubbles in real time remains. In summary, GBAS can benefit from an additional constellation like Galileo, as concluded by Caamano *et al.* (2016).

The dual frequency approach to GBAS is based on the use of the new GPS L5 signal and/or the Galileo E5 signal in addition, respectively, to GPS L1 and Galileo E1. One feature of this approach is the use of ionosphere-free observables, meaning range measurements from which ionospheric delay is removed (to first order), which effectively eliminates the gradient threat. For this approach, a baseline algorithm and nominal performance estimation can be found in Gerbeth *et al.* (2016). A summary of the calculation of the ionosphere-free observable is presented here using smoothed code pseudoranges for GPS L1 and L5, for example ($\rho_{Ifree,L1L5}$), given by:

$$\rho_{Ifree,L1L5} = \frac{f_{L1}^2\,\rho_{L1} - f_{L5}^2\,\rho_{L5}}{f_{L1}^2 - f_{L5}^2} \tag{6}$$

where f_{L1} and f_{L5} are respectively the GPS L1 and L5 center frequencies and ρ_{L1} and ρ_{L5} are the smoothed pseudorange measurements for these two frequencies, respectively.

With the ionosphere-free combination calculated in the airborne, the ionospheric gradient component of the term σ_{vig} is negligible, and geometry screening in the ground station is no longer necessary, since no significant ionospheric decorrelation between ground and airborne remains. However, by combining code measurements from two frequencies, the output code noise and multipath error is magnified, resulting in larger position errors.

Considering the ionospheric delays at L1 and L5 respectively as I_{L1} and I_{L5} and the signal frequencies f_{L1} and f_{L5} respectively as 1,575.42 and 1,176.45 MHz, the ionospheric delay at L5 is given by (Gerbeth *et al.* 2016):

$$I_{L5}f_{L5}^2 = I_{L1}f_{L1}^2 \Rightarrow I_{L5} = \frac{f_{L1}^2}{f_{L5}^2}I_{L1} \Rightarrow I_{L5} = 1.79\,I_{L1} \tag{7}$$

Hence, in this case, the ionospheric delay in L5 is increased by a factor of almost 1.8. Also, considering, for example, the term σ_{air} in Eq. 3, which accounts for code noise and multipath, the standard deviation of errors in airborne range measurements using the ionosphere-free combination with L1 and L5 is given by Felux *et al.* (2017a) under the assumption that the two signals have statistically independent errors (which is untrue but conservative, as multipath errors are positively correlated across frequency):

$$\sigma_{air,Ifree} = \sqrt{\left(\frac{f_{L1}^2}{f_{L1}^2 - f_{L5}^2}\right)^2 \sigma_{air,L1}^2 + \left(\frac{f_{L5}^2}{f_{L1}^2 - f_{L5}^2}\right)^2 \sigma_{air,L5}^2} \tag{8}$$

A similar increase as that expressed by Eq. 8 would take place in the ground system error (σ_{pr_gnd}) for the same reason. Hence, the use of ionosphere-free observables in position solutions and the computation of protection levels results in worse nominal performance in terms of accuracy and availability. Also, in this approach, it is necessary to keep continuous tracking of the signals simultaneously on both frequencies. For this reason, Felux *et al.* (2017a) argued that there is no significant benefit to using ionosphere-free mode under ionospheric scintillation. In the presence of scintillation, the probability of tracking both signals is lower than tracking just the L1 signal (L5, being at a lower frequency, is more susceptible to the behavior that causes scintillation).

The fact that scintillation over low-latitude regions affects more prominently the L5 signal is a concern for using this frequency. Recently, the work of Salles *et al.* (2021a) showed larger probabilities of strong scintillation events for the L5 signal when compared to the L1. Under specific scenarios, these probabilistic ratios exceed a factor of five. Additionally, Salles *et al.* (2021b) showed that the cases of scintillation with –15 dB fading events are much more common in the L5 signal, with approximately 2.5 times more occurrences of this type for S_4 in L1 of 0.8, increasing potential to availability issues. Salles *et al.* (2021b) also showed that the deepest fading of the L5 signal reaches values close to twice those values from the L1 signal. These results agree with the statistical analysis presented by Moraes *et al.* (2018), where evidence for more severe fading occurrences in the L5 were found.

As a conclusion for ionosphere-free observables in position solutions, Felux *et al.* (2017a) suggest using the ionosphere-free mode solely for monitoring gradient threats while calculating position solutions using the single-frequency approach with two GNSS constellations, if available. Extending this concept, Felux *et al.* (2017b) present a method in which gradients are monitored by having each aircraft comparing ionospheric delay estimates from the ground station with those that it estimates. The authors argue that this approach to sharing the responsibility of monitoring threatening gradients between the ground facility and the airborne subsystem is less conservative and more realistic.

Note that there are limitations on the capacity of the GBAS VDB (Stanisak *et al.* 2015). Currently, there is no space in the VDB messages to transmit ionospheric delays estimated by the ground station. For this reason, in the method proposed by Felux *et al.* (2017b), which is improved and tested by Felux *et al.* (2019), the test statistic for ionospheric gradient monitoring uses the pseudorange corrections broadcast for each frequency. In this way, ionospheric delays affecting both the ground and the aircraft are estimated by the airborne subsystem using a quantity called pseudo ionospheric delay. The details about this monitoring strategy are found in Felux *et al.* (2016; 2017b; 2019). Note that each aircraft is required to make its own ionospheric integrity determination because, while it obtains pseudorange corrections from the ground, it has no means to provide its measurements or delay estimates back to the ground station (i.e., the GBAS VDB only communicates information in one direction, from ground to aircraft).

In summary, ionospheric mitigation for GBAS using dual-frequency measurements does not provide a simple solution and presents advantages and disadvantages that must be taken into account when defining the specific algorithm and mitigation strategy to be used. At the present time, the details of how future GBAS will apply dual frequency and multi-constellation measurements remain unclear.

FINAL REMARKS

In a series of survey papers of which this is the first, the main goal of this first part is to provide an overview of the most relevant aspects of GBAS technology along with the main challenges for its operation in low-latitude regions, specifically in Brazil. Due to the strong influence of the ionosphere, the physics and drivers of the most relevant phenomena in low latitudes will be discussed in the subsequent paper of this series. Given how vast the subject is, this paper has not covered any particular topic in depth. Instead, it has provided a general view to the reader not entirely familiar with how GBAS works and the main issues with making this technology operational and cost-effective in Brazil.

Since large ionospheric spatial gradients are both more severe and more common in Brazil than in midlatitudes, it is much harder to provide high availability of GBAS-supported precision approaches at local nighttime in Brazil, when these large gradients are a threat. This paper has explained the basis for determining the availability and integrity of GBAS in terms of computing PL bounds on rare-event GBAS position errors and confirming in real time that these error bounds are smaller than the safety limits (ALs) that apply to the operation being conducted. It has also given an overview of techniques for geometry screening that must be applied to protect existing GBAS PA users from worst-case ionospheric gradients. Geometry screening significantly degrades PA (but not NPA) availability, and this degradation is what currently prevents useful CAT I or better service from being provided in Brazil (at least at nighttime).

To provide a perspective on the future of GBAS in Brazil, the dual frequency and dual-constellation strategy for GBAS was also described with its advantages and disadvantages. Considering all the findings and conclusions, the dual frequency/dual constellation approach appears to be the only way Brazil can benefit from GBAS sufficiently to make its installation worthwhile.

AUTHORS' CONTRIBUTION

Conceptualization: Moraes AO, Marini-Pereira L Sousasantos J and Pullen S; **Investigation:** Marini-Pereira L and Pullen S; **Methodology:** Marini-Pereira L and, Pullen and Moraes AO; **Resources:** Pullen S; **Writing – original draft:** Marini-Pereira L and Pullen S; **Writing – review & editing:** Pullen S; Sousasantos J and Moraes AO.

DATA AVAILABILITY STATEMENT

Not applicable.

FUNDING

ACKNOWLEDGEMENTS

REFERENCES

[DECEA] Departamento de Controle do Espaço Aéreo (2020) GeoServer. Visualizador de camada. DECEA. [accessed Dec 9 2020]. https://geoaisweb.decea.mil.br/geoserver/web/wicket/bookmarkable/org.geoserver.web.demo.MapPreviewPage?0

[ICAO] International Civil Aviation Organization (2002) RLA/00/009 Project: Second Coordination Meeting on GNSS Augmentation Trials. Montreal: ICAO. [accessed Oct 2 2021]. https://www.icao.int/SAM/Documents/2002/GNSSA2/GNSSAII_WP04.pdf

[ICAO] International Civil Aviation Organization (2006) RLA/00/009 Project: GNSS Augmentation Tests, Final Report. Montreal: ICAO. [accessed Oct 2 2021]. https://www.icao.int/SAM/eDocuments/RLA00009_ProjectFinalReport.pdf

[ICAO] International Civil Aviation Organization (2014) Doc 9613, Performance-based Navigation (PBN) Manual. 4 ed. 2013. Amendment 1, January 24th, 2014.

[ICAO] International Civil Aviation Organization (2020b) Annex 10 to the Convention on International Civil Aviation, Aeronautical Telecommunications Volume I: Radio Navigation Aids, 7. ed. July, 2018. Amendment 92, November 5th, 2020. Montreal: ICAO.

[ICAO] International Civil Aviation Organization (2020a) Doc 8168, Procedures for Air Navigation Services: Aircraft Operations Volume I: Flight Procedures. Montreal: ICAO.

[RTCA] Radio Technical Commission for Aeronautics (2004) SC-159 DO 245A: Minimum aviation system performance standards for the local area augmentation system (LAAS). Washington: RTCA.

[RTCA] Radio Technical Commission for Aeronautics (2008) SC-159 DO 253C: Minimum operational performance standards for GPS/Local Area Augmentation System Airborne Equipment. Washington: RTCA.

[RTCA] Radio Technical Commission for Aeronautics (2017) SC-159 DO 253D: Minimum Operational Performance Standards for GPS/Local Area Augmentation System Airborne Equipment. Washington: RTCA.

Belabbas B, Remi P, Meurer M, Pullen S (2011) Absolute slant ionosphere gradient monitor for GAST-D: Issues and opportunities. Paper presented 24th International Technical Meeting of the Satellite Division of The Institute of Navigation (ION GNSS 2011). ION; Portland, Oregon, United States of America.

Blanch J, Walter T, Enge P (2019) Gaussian bounds of sample distributions for integrity analysis. IEEE Trans Aerosp Electron Syst 55(4):1806-1815. https://doi.org/10.1109/TAES.2018.2876583

Caamano M, Felux M, Circiu MS, Gerbeth D (2016) Multi-constellation GBAS: How to benefit from a second constellation. Paper presented 2016 IEEE/ION Position, Location and Navigation Symposium (PLANS). IEEE; Savannah, Georgia, United States of America. https://doi.org/10.1109/PLANS.2016.7479779

Caamano M, Miguel Juan J, Felux M, Gerbeth D, González-Casado G, Sanz J (2021) Network-based ionospheric gradient monitoring to support GBAS. Navigation 68(1):135-156. https://doi.org/10.1002/navi.411

Chang H, Yoon M, Lee J, Pullen S, Marini-Pereira L (2019) Assessment of ionospheric spatial decorrelation for daytime operations of GBAS in the Brazilian region. Paper presented 2019 International Technical Meeting of The Institute of Navigation (ION ITM 2019). ION; Reston, Virginia, United States of America. https://doi.org/10.33012/2019.16673

Chang H, Yoon M, Pullen S, Marini-Pereira L, Lee J (2021) Ionospheric spatial decorrelation assessment for GBAS daytime operations in Brazil. Navigation 68(2):391-404. https://doi.org/10.1002/navi.418

Datta-Barua S, Lee J, Pullen S, Luo M, Ene A, Qiu D, Zhang G, Enge P (2010) Ionospheric threat parameterization for local area global-positioning-system-based aircraft landing system. J Aircr 47(4):1141-1151. https://doi.org/10.2514/1.46719

Dautermann T, Felux M, Grosch A (2012) Approach service type D evaluation of the DLR GBAS testbed. GPS Solut 16:375-387. https://doi.org/10.1007/s10291-011-0239-3

Felux M, Circiu MS, Gerbeth D, Caamano M, Stanisak M (2016) Ionospheric monitoring in a dual frequency GBAS. Paper presented 2016 IEEE Aerospace Conference. IEEE; Big Sky, Montana, United States of America. https://doi.org/10.1109/AERO.2016.7500884

Felux M, Circiu MS, Gerbeth D, Caamano M (2017a) Future GBAS processing: Do we need an ionosphere-free mode? Paper presented International Symposium on GNSS (ISGNSS 2017). ISGNSS; Hongkong, China. [accessed Jun 8 2020]. https://elib.dlr.de/117741/1/Paper_Felux.pdf

Felux M, Circiu MS, Lee J, Holzapfel F (2017b) Ionospheric gradient threat mitigation in future dual frequency GBAS. Int J Aerosp Eng 2017:4326018. https://doi.org/10.1155/2017/4326018

Felux M, Caamano M, Circiu MS, Gerbeth D (2019) Improved ionospheric monitoring for future dual-frequency GBAS. Paper presented International Symposium on Global Navigation Satellite System 2019. ISGNSS; Jeju, South Korea. [accessed Jun 8 2020]. https://elib.dlr.de/130212/1/ISGNSS_Full_Paper_Felux.pdf

Gerbeth D, Circiu MS, Caamano M, Felux M (2016) Nominal performance of future dual frequency dual constellation GBAS. Int J Aerosp Eng 2016:6835282. https://doi.org/10.1155/2016/6835282

GPS World GNSS Positioning Navigation Timing (2021) The almanac: Orbit data and resources on active GNSS satellites. GPS World. [accessed Aug 6 2021]. https://www.gpsworld.com/the-almanac/

Hatch R (1982) The synergism of GPS code and carrier measurements. Paper presented International Geodetic Symposium on Satellite Doppler Positioning. SAO/NASA; Las Cruces, New Mexico, United States of America.

Hofmann-Wellenhof B, Lichtenegger H, Wasle H (2008) GNSS: Global navigation satellite system: GPS, GLONASS, Galileo and more. Vienna: Springer-Verlag.

Jing J, Khanafseh S, Langel S, Chan FC, Pervan B (2015) Optimal antenna topologies for spatial gradient detection in differential GNSS. Radio Sci 50:728-743. https://doi.org/10.1002/2014RS005646

Khanafseh S, Pullen S, Warburton J (2012) Carrier phase ionospheric gradient ground monitor for GBAS with experimental validation. Navigation 59(1):51-60. https://doi.org/10.1002/navi.3

Ko P (2000) GPS-based precision approach and landing navigation: Emphasis on inertial and pseudolite augmentation and differential ionosphere effect (doctoral dissertation). Stanford: Stanford University.

Larson JD, Gebre-Egziabher D, Rife JH (2019) Gaussian-Pareto overbounding of DGNSS pseudoranges from CORS. Navigation 66(1):139-150. https://doi.org/10.1002/navi.276

Lee J (2005) GPS-based aircraft landing systems with enhanced performance: Beyond accuracy (doctoral dissertation). Stanford: Stanford University. In English.

Lee J, Pullen S, Datta-Barua S, Enge P (2007) Assessment of ionosphere spatial decorrelation for global positioning system-based aircraft landing systems. J Aircr 44(5):1662-1669. https://doi.org/10.2514/1.28199

Lee J, Seo J, Park YS, Pullen S, Enge P (2011) Ionospheric threat mitigation by geometry screening in ground-based augmentation systems. J Aircr 48(4):1422-1433. https://doi.org/10.2514/1.C031309

Lee J, Yoon M, Pullen S, Gillespie J, Mather N, Cole R, Souza JR, Doherty P, Pradipta R (2015) Preliminary results from ionospheric threat model development to support GBAS operations in the Brazilian region. Paper presented 28th International Technical Meeting of The Satellite Division of the Institute of Navigation (ION GNSS+ 2015). ION; Tampa, Florida, United States of America.

Mayer C, Belabbas B, Jakowski N, Meurer M, Dunkel W (2009) Ionosphere threat space model assessment for GBAS. Paper presented 22nd International Technical Meeting of the Satellite Division of The Institute of Navigation (ION GNSS 2009). ION; Savannah, Georgia, United States of America.

Mirus Technology (2015) Effects of low latitude ionospheric activity on global navigation satellite systems (GNSS). Final report of project funded by USTDA. [accessed May 30 2021] https://www.icao.int/SAM/Documents/2016-PBNGNSS/Low%20Latitude%20Threat%20Model-Final-Jan15.pdf

Moraes AO, Vani BC, Costa E, Sousasantos J, Abdu MA, Rodrigues F, Gladek YC, Oliveira CBA, Monico JFG (2018) Ionospheric scintillation fading coefficients for the GPS L1, L2, and L5 frequencies. Radio Sci 53(9):1165-1174. https://doi.org/10.1029/2018RS006653

Murphy T, Harris M, Shively C, Azoulai L, Brenner M (2012) Fault monitoring for GBAS airworthiness assessments. Navigation 59(2):145-161. https://doi.org/10.1002/navi.12

Pullen S, Enge P (2007) An overview of GBAS integrity monitoring with a focus on ionospheric spatial anomalies. Indian J Radio Space Phys 36:249-260.

Pullen S, Luo M, Walter T, Enge P (2010) Using SBAS to enhance GBAS user availability results and extensions to enhance air traffic management. Paper presented 2nd ENRI International Workshop on ATM/CNS (EIWAC 2010). EIWAC, Tokyo, Japan. [accessed Jul 27 2018]. http://www-leland.stanford.edu/~spullen/SBAS%20to%20GBAS%20Network%20Benefits%20EIWAC-10.pdf

Pullen S (2017) Ground based augmentation systems. In: Teunissen PJG, Montenbruck O, editors. Springer Handbook of Global Navigation Satellite Systems. Basingstoke: Springer. p. 905-932. https://doi.org/10.1007/978-3-319-42928-1_31

Pullen S, Cassell R, Johnson B, Brenner M, Weed D, Cypriano L, Topland M, Stakkeland M, Pervan B, Harris M, *et al.* (2017) Impact of ionospheric anomalies on GBAS GAST D service and validation of relevant ICAO SARPs requirements. Paper presented 30th International Technical Meeting of the Satellite Division of The Institute of Navigation (ION GNSS+ 2017). ION; Portland, Oregon, United States of America. https://doi.org/10.33012/2017.15135

Ramakrishnan S, Lee J, Pullen S, Enge P (2008) Targeted ephemeris decorrelation parameter inflation for improved LAAS availability during severe ionosphere anomalies. Paper presented 2008 National Technical Meeting of The Institute of Navigation. ION; San Diego, California, United States of America.

Reuter R, Weed D, Brenner M (2012) Ionosphere gradient detection for Cat III GBAS. Paper presented 25th International Technical Meeting of the Satellite Division of The Institute of Navigation: 2175-2183. ION; Nashville, Tennessee, United States of America.

Robert E, Jonas P, Vuillaume J, Salos D, Hecker L, Yaya P (2018) Development of a European ionosphere threat model in support of GBAS deployment. Paper presented 2018 IEEE/ION Position, Location and Navigation Symposium (PLANS). IEEE; Monterey, California, United States of America. https://doi.org/10.1109/PLANS.2018.8373503

Saito S, Yoshihara T, Nakahara H (2015) Performance of GAST-D ionospheric gradient monitor studied with low latitude ionospheric disturbance data obtained in a real airport environment. Paper presented ION 2015 Pacific PNT Meeting. ION; Honolulu, Hawaii, United States of America.

Salles LA, Vani BC, Moraes A, Costa E, Paula ER (2021a) Investigating ionospheric scintillation effects on multifrequency GPS signals. Surv Geophys 42:999-1025. https://doi.org/10.1007/s10712-021-09643-7

Salles LA, Moraes A, Vani BC, Sousasantos J, Affonso BJ, Monico JFG (2021b) A deep fading assessment of the modernized L_2C and L_5 signals for low-latitude regions. GPS Solut 25:122. https://doi.org/10.1007/s10291-021-01157-4

Seo J, Lee J, Pullen S, Enge P, Close S (2012) Targeted parameter inflation within ground-based augmentation systems to minimize anomalous ionospheric impact. AIAA J Aircr 49(2):587-599. https://doi.org/10.2514/1.C031601

Shively CA, Niles R (2008) Safety concepts for mitigation of ionospheric anomaly errors in GBAS. Paper presented 2008 National Technical Meeting of The Institute of Navigation. ION; San Diego, California, United States of America.

Stanisak M, Lipp A, Feuerle T (2015) Possible VDB formatting for multi-constellation / multi-frequency GBAS. Paper presented 28th International Technical Meeting of the Satellite Division of The Institute of Navigation (ION GNSS+ 2015). ION; Tampa, Florida, United States of America.

Tang H, Walter T, Blanch J, Enge P, Chan F-C (2009) Flight test data validation of dual-frequency GPS measurement error characteristics. Paper presented 22nd International Technical Meeting of the Satellite Division of The Institute of Navigation (ION GNSS 2009). ION; Savannah, Georgia, United States of America.

van Graas F, Zhu Z (2011) Tropospheric delay threats for the ground based augmentation system. Paper presented 2011 ION International Technical Meeting (ITM). ION; San Diego, California, United States of America.

Xie G (2003) Optimal on-airport monitoring of the integrity of GPS-based landing systems (doctoral dissertation). Stanford: Stanford University. In English.

Yoon M, Kim D, Lee J, Pullen S (2015) Multi-dimensional verification methodology of ionospheric gradient observation during plasma bubble events in the Brazilian region. Paper presented ION 2015 Pacific PNT Meeting. ION; Honolulu, Hawaii.

Yoon M, Kim D, Lee J, Rungruengwajiake S, Pullen S (2016) Assessment of equatorial plasma bubble impacts on ground-based augmentation systems in the Brazilian region. Paper presented 2016 International Technical Meeting of The Institute of Navigation. ION; Monterey, California, United States of America. https://doi.org/10.33012/2016.13423

Yoon M, Lee J, Pullen S, Gillespie J, Mathur N, Cole R, Souza JR, Doherty P, Pradipta R (2017a) Equatorial plasma bubble threat parameterization to support GBAS operations in the Brazilian region. Navigation 64(3):309-321. https://doi.org/10.1002/navi.203

Yoon M, Kim D, Lee J (2017b) Validation of ionospheric spatial decorrelation observed during equatorial plasma bubble events. IEEE Trans Geosci Remote Sens 55(1):261-271. https://doi.org/10.1109/TGRS.2016.2604861

Yoon M, Kim D, Lee J (2020) Extreme ionospheric spatial decorrelation observed during the March 1, 2014, equatorial plasma bubble event. GPS Solut 24:47. https://doi.org/10.1007/s10291-020-0960-x